BNL 31797

Conf-820735--6

BNL--31797

DE83 000217

August 1982

MASTER

Recent Progress in Commensurate-Incommensurate Phase Transformations

J. D. Axe

NOTICE
PORTIONS OF THIS REPORT ARE ILLEGIBLE. It Has Been Reproduced From The Best Available Copy To Permit The Broadest Possible Availability.

DISCLAIMER

This report was prepared as an account of work sponsored by an agency of the United States Government. Neither the United States Government nor any agency thereof, nor any of their employees, makes any warranty, express or implied, or assumes any legal liability or responsibility for the accuracy, completeness, or usefulness of any information, apparatus, product, or process disclosed, or represents that its use would not infringe privately owned rights. Reference herein to any specific commercial product, process, or service by trade name, trademark, manufacturer, or otherwise, does not necessarily constitute or imply its endorsement, recommendation, or favoring by the United States Government or any agency thereof. The views and opinions of authors expressed herein do not necessarily state or reflect those of the United States Government or any agency thereof.

The submitted manuscript has been authored under contract DE-AC02-76CH00016 with the Division of Basic Energy Sciences, U.S. Department of Energy. Accordingly, the U.S. Government retains a nonexclusive, royalty-free license to publish or reproduce the published form of this contribution, or allow others to do so, for U.S. Government purposes.

DISTRIBUTION OF THIS DOCUMENT IS UNLIMITED

BNL 31797

Recent Progress in Commensurate-Incommensurate Phase Transformations

J. D. Axe

Brookhaven National Laboratory

Upton, New York 11973 USA

ABSTRACT: Three topics are discussed. i) The nature of long wavelength excitations in $Hg_{3-\delta}AsF_6$, where gapless excitations in addition to the conventional acoustic modes are observed. ii) Thiourea, in which new commensurate phases can be induced by an external electric field. iii) Discommensurations in $2HTaSe_2$, where recent electron diffraction and high resolution x-ray data combine with neutron results to establish a quite complex and subtle behavior.

There have been many interesting studies of incommensurate systems in the past few years, many of them involving either elastic and/or inelastic neutron scattering. In a short review it would not be possible to summarize even a substantial fraction of them in a meaningful way. Instead I have chosen three topics that I have some familiarity with and for which neutrons have played a key role in our present understanding.

I. Long wavelength excitations in incommensurate intergrowth compounds.

We define an incommensurate intergrowth compound as one composed of two (or more) interpenetrating sublattices with incommensurate lattice spacings. The incommensurability is of degree d ($1<d<3$) if the lattices are incommensurate along d independent directions. If the intersublattice forces are short ranged and if surfaces are neglected (periodic boundary conditions), for sufficiently weak interactions and spacings sufficiently far away from commensurability the total energy of the system is unchanged upon sliding one sublattice along an incommensurate direction with respect to the other sublattice(s). As a result there are 3+d gapless long wavelength excitations (Goldstone modes) in place of the conventional three acoustic branches. Some of the expected features of these excitations have been previously discussed. [1]

The most studied and consequently best understood d=1 example is the linear chain mercury compound $Hg_{3-\delta}AsF_6$, [2]-[4]. (See Fig. 1). Heilmann, et.al., [4], in the course of a more extensive investigation measured the dispersion of some low frequency phonons emanating from the AsF_6 sublattice Bragg peaks in $Hg_{3-\delta}AsF_6$. They noted that whereas in conventional elastic media the sound velocity, $v(\vec{q}\parallel\vec{a},\vec{e}\parallel\vec{c})=\vec{v}(\vec{q}\parallel\vec{c},\vec{e}\parallel a)\sqrt{c_{44}}$, in $Hg_{3-\delta}AsF_6$

$$R(\text{meas.}) \equiv \frac{v(\vec{q}\parallel\vec{a};\vec{e}\parallel\vec{c})}{v(\vec{q}\parallel\vec{c};\vec{e}\parallel\vec{a})} = 1.25\ (\pm.1) \qquad (1)$$

Axe and Bak [5] have considered the long wave lattice dynamics of $Hg_{3-\delta}AsF_6$ from the viewpoint of continuum elastic theory. They define five "slow" collective coordinates

$$u_x = 1/2(u_x^A + u_x^Y)$$

$$u_y = 1/2(u_y^A + u_y^X)$$

$$u_z = 1/3(u_z^A + u_z^X + u_z^Y) \qquad (2)$$

$$w_x = u_x^X$$

$$w_y = u_y^Y$$

Here the superscript A denotes the AsF_6 sublattice, and the superscript X(Y) denotes the Hg-chain sublattice oriented along the X(Y) axis. As in conventional elastic theory the elastic energy, U, is expressed in terms of the quadratic products of the spatial gradients of the slow coordinates. In addition to the point group symmetry restrictions on the form of $U(\partial_i u_j; \partial_k w_\ell)$, all the terms involving $\partial_{y,z} w_x$ and $\partial_{x,z} w_y$ vanish above T_c=120K, at which temperature each Hg sublattice "melts", leaving a collection of individual independent 1d Hg chains, whose properties have been measured [2]-[4], and discussed by Emery and Axe [6]. Thirteen non-equivalent terms, each multiplied by a generalized elastic constants serve to describe U.

Not enough experimental data exist to fix all of the constants but the velocities for propagation along the x- and z-axes for all five branches exist [4]. When the elastic energy is fitted to these data, the behavior of the variation of velocity with propagation direction is as shown in Fig. 2. For $\vec{q} \parallel \vec{a}$ there are two (mixed) longitudinal modes involving u_x and w_x. The high velocity mode (large contribution from w_x) predominantly propagates on the Hg chains, while the low velocity mode involves mostly the AsF_6 sublattice. Of the remaining three transverse modes, one, involving only the shear $\partial_x w_y$ has a

vanishing velocity and is purely diffusive in character ($\omega(q)$ $i\eta q^2$, where η is an appropriate viscosity). For $q \parallel c$ there is one longitudinal mode (u_z), two degenerate transverse modes (u_x, u_y) and two zero velocity Hg-shear modes (w_x, w_y). One mode (w_y) is in fact diffusive everywhere in the (x,z) plane.

In spite of the large number of elastic constants necessary for a general treatment, it is possible to discuss the failure of the conventional elastic relation R=1 pointed out above in exact and simple terms. The two shear strains under discussion are shown schematically in Fig. 3. The key point is that in Fig. (3a) all displacements are along c, for which both Hg-sublattices and the AsF_6 sublattice are coupled. The shearing of the Hg-sublattices do not contribute to the elastic stiffness but do contribute to the inertial mass. By contrast the a-axis displacements of the AsF_6 (Fig. 3b) couples only to one of the Hg-sublattices, the x-axis array being free relative to displacements along x. Consequently only one of the two Hg-sublattices participates in this mode. Both modes have the same elastic stiffness, so it follows trivially that

$$R = \left(\frac{\rho_A + 2\rho_{Hg}}{\rho_A + \rho_{Hg}}\right)^{1/2} = 1.27 \qquad (3)$$

where ρ_A and ρ_{Hg} are respectively the mass density of the AsF_6 and the Hg-sublattices. The agreement between observed and calculated R-values provides a direct and striking demonstration of the ability of two incommensurate sublattices to slide freely relative to one another. Further low frequency acoustic and/or light scattering studies of the unusual low frequency long wavelength modes of incommensurate intergrowth compounds should prove rewarding.

II. Thiourea

Thiourea is one of the first known examples of an insulator with a commensurate-incommensurate phase transformations. [7] Above T_o=218K (see Fig. 1) it is non polar orthorhombic (space group Pnma) [8]. Below T_c=191K [the values of T_o and T_c refer to the deuterated material] the n-glide is lost essentially by virtue of a tilting of the planar thiourea molecules about the b-axis, resulting in a ferroelectric with a-axis polarization. [9] Between T_o and T_c, sattelite reflections of the type $(h,k+n\delta,\ell)$ reveal b-axis modulation of the polarization (h,k,ℓ,n=integers; δ=modulation wavevector). [8],[10] Fig. 4 shows the P-T phase diagram as determined by a recent neutron study by Denoyer, et.al. [11] At ambient pressure the δ=0 and δ=1/9 commensurate phases are stable in addition to an incommensurate phase ($.141>\delta(T)>.115$). Increased pressure stabilizes two new δ=1/7 and δ=1/3 phases.

One point which immediately arises on inspection of Fig. 4 is the absence of even order commensurate phases. Denoyer, et.al. [11] showed that this is a simple consequence of symmetry. If P_δ represents the amplitude of the primary sinusoidally modulated polarization with wave vector $\vec{q}_\delta$, the lowest order commensurate lock-in potential of order n in a Landau free-energy expansion involves the n-th order anharmonic potential $V_n(P_\delta^n+P_{-\delta}^n)$ and translation symmetry demands that $n\vec{q}_\delta=mb^*=\vec{G}$ (a reciprocal lattice vector). Denoyer, et.al. [11] showed that for thiourea point symmetry requires that m and n be of the same parity. Thus for example δ=1/7 and 1/9 lock in require seventh and ninth order anharmonic terms, whereas δ=1/8 involves the much weaker 16'th order coupling and is not seen. However Denoyer et.al.[11] were clever enough to realize that another way to stabilize δ=1/8

superstructure was through, for example, symmetry allowed terms of the form

$$V_8' P_o (P_\delta^8 + P_{-\delta}^8) \propto \chi_o E (P_\delta^8 + P_{-\delta}^8) \tag{4}$$

where P_o is the macroscopic polarization along the a-axis which can be induced through an electric field E through the $\vec{q}=0$ susceptibility χ_o. This raises the possibility of an electric field induced $\delta=1/8$ commensurate phase in thiourea.

That this possibility is indeed realized was inferred in a dielectric susceptibility study of Jamet, et.al., [12] and directly confirmed in an elastic neutron study by Moudden, et.al.[13] Under the assumption that the polarization near $\delta=1/8$ lock in is phase modulated, i.e. that P(y) is given by

$$P(y) = A\exp i\left[\frac{1}{8}b^* y + \phi(y)\right] \tag{5}$$

the simplest Landau free energy which describes the basic features is of the sine-Gordon type

$$\nabla F = \int dy\left\{\frac{1}{2}\alpha A^2 + \frac{1}{4}\beta A^4 + \frac{1}{2}\beta\left(\nabla\phi - q_o(T)\right)^2 A^2 + V_8' \chi E A^8 \cos^8\phi\right\}. \tag{6}$$

To lowest order in $\sqrt{E}$ a commensurate phase minimizes eqn. 6 over a range of temperatures $T_- < T < T_+$ with $T_\pm$ given by

$$T_\pm = T_8 \pm \text{const.}\ \sqrt{E}\ . \tag{7}$$

Figure 5 shows the effect of an applied E field on the variation of $\delta(T)$ as determined by the elastic neutron study.[13] The behavior of $T_\pm(E)$ is in agreement with that deduced from the dielectric study [12] which is in turn in agreement with eqn. 7 for $|E| < 10^3$V/cm. These measurements represent the first example of the control of the lock-in potential by an externally variable field. Such systems should prove very valuable in future studies of discreteness effects (e.g. devils staircases). These effects are expected to become important for thiourea only for much higher fields.

III. Phase Transformations and Discommensurations in $2HTaSe_2$

Of the various quasi 2-d CDW systems, the 2H polytype of $TaSe_2$ has been most thoroughly investigated.[14] The system is very rich in the sense that each increase in the resolution or sophistication of the probe has uncovered more subtle behavior. Early electron diffraction studies showed sattelite reflections appearing at $T<T_o=123K$ [14]. Initially these peaks were thought to be commensurate, with reduced wave vector $\vec{q}_c=\vec{a}^*/3$, but a subsequent higher resolution neutron scattering study by Moncton, et.al., [15] showed structure to be incommensurate near T_o with wave vector $\vec{q}_\delta=(1-\delta)\vec{a}^*/3$. δ, initially $\approx .02$, was shown to vary smoothly upon cooling until $T_c=90K$ where δ went rapidly to zero. Both the incommensurate and commensurate phases exhibited hexagonal symmetry on a macroscopic scale. Moncton, et.al.[15] went on to study the temperature dependent amplitude of the CDW and the dynamics of the transformation as well as to discuss the mechanism for $\delta(T)$ and the ultimate "lock in" transformation, $\delta(T)\rightarrow 0$.

The next discovery came in a high resolution xray study by Fleming et.al.[16], who found a new incommensurate CDW structure which could only be obtained upon warming and which manifested itself through a splitting of the CDW sattelites on a scale unresolved in the previous studies. This new phase was stable on warming from T_{CS} to $T_{SI}=112K$ and displayed a clear lack of hexagonal symmetry. (See Fig. 6). Unlike the commensurate and the fully incommensurate states discussed above where the modulation is a coherent superposition of <u>identical</u> components with wave vectors, $(\vec{q}_1,\vec{q}_2,\vec{q}_3)$, along each of the three trigonal symmetry axes, the new phase had three coexisting <u>nonequivalent</u> wave vectors, one of which remained commensurate. Whereas the fully incommensurate phase can be thought of as characterized by commensurate regions separated by a hexagonal (honeycomb) pattern of domain

walls or discommensurations (DC's), the three nonequivalent wavevectors implied a linear or striped arrangement of DC's. The relative stability of striped vs. hexagonal domain patterns had been previously discussed by Bak et.al. [17], and rests (at T=0) on a competition between wall touching energy (nonexistent for a stripe phase) and wall-wall repulsion (for the same density of parallel DC's, they are further apart for the honeycomb). At finite temperatures there is a greater entropy associated with the honeycomb. Thus below T_{SH} the fully incommensurate phase is metastable and the transformation is discontinuous as predicted theoretically.[17] The onset transformation at T_o appears continuous but is expected to be 1st order. The transformations [at T_{CI} (on cooling) and T_{CS} (on warming)] appear continuous but only the latter is predicted to be so.

The next round at revelations came from the direct imaging of domain microstructure using superlattice dark field electron microscopy. [18,19] The first surprise was that the commensurate phase although hexagonal on a macroscopic scale consists of rather large (≈1μm) domains having orthorhombic symmetry. The explanation of the broken hexagonal symmetry is rather subtle. If the distortions for a single $TaSe_2$ layer are analyzed assuming the superposition of three plane wave CDW's with amplitudes $\psi_j = ae^{i\phi_j}$ (j=1,3 associated with the equivalent wavevectors $\vec{q}_j$) three possible structures are possible. [20],[21] (See Fig. 7). The different choices for ϕ_j are reflected by a shifting of the position of the 3-fold axis within a single layer. In each case the distorted layer retains hexagonal symmetry, but there are two layer per unit cell and the resultant pattern can have lower symmetry. It is found that 3-d structures built from type-I layers is hexagonal but those built from type-II and -III layers are orthorhombic.[20] Such an orthorhombic cell can be

oriented in three different ways on a hexagonal lattice thus accounting for the domains and it appears that only the type-II structure is compatible with NMR [22] and Mossbauer [23] studies as well as the electron microscopy.

Beautiful confirmation of McMillan's [24] proposal of the importance of DC's in the incommensurate phases is obtained by the electron microscope studies. On warming above T_{CS} alternate regions of dark and bright stripes nucleate within each orthorhombic domain. (See Fig. 8) The average width, L, of the stripes changes with temperature in agreement the xray diffraction measurement of the incommensurability δ ($L=2\pi/3\delta$). The dark and bright stripes represent domains of differently oriented orthorhombic material and the discommensurations (boundaries between the dark and bright stripes) are narrower than instrumental resolution (50Å). The stripes are observed often to annihilate at a node (called a CDW dislocation) in which exactly six discommensurations disappear. Several models have been proposed to account for these observations.Perhaps the most appealing scheme is that proosed by Walker and Jacobs [25] in which linear discommensurations in odd layers (DC_-) lie exactly halfway between those (DC_+) in the even layers. The resulting 3d pattern is of alternating stripes of orthorhombic phase with two different orientations representing the light and dark stripes, respectively. The fact that a CDW dislocation involves six DC's is related to the fact the CDW in each layer undergoes a phase change of $2\pi/3$ at a DC and so changes by 2π in a loop enclosing the dislocation.

The direct imaging of the high temperature incommensurate phase (cooling below T_0 or warming above T_{SI}) is more ambiguous, in part due to resolution problems attendant with the fineness of the domain spacings at high temperatures. [18],[19] The resulting patterns [18] [19] seem consistent with a (double) the hexagon honeycomb array as partly anticipated by xray and neutron diffraction studies and as predicted by theory [20] [21].

Returning finally to neutron and xray studies, McWhan et.al. [26],[27] have investigated the effect of hydrostatic pressure on the CDW phases. The results are shown in Fig. 9. Pressure destabilizes the commensurate phase and then, surprisingly, restabilizes a (different?) commensurate phase. There are at yet no measurements which differentiate the high and low pressure commensurate phases, but there is some theoretical indication of the sort of added complexity which may be expected. Littlewood and Rice [21] have considered a model in which the energies of type I and type II single layer patterns are nearly equal. As a result i) domain walls (DC's) separating two type II regions can be "decorated" with an intervening type I region, thereby lowering its formation energy; ii) the reduced energy of such a DC destabilizes the orthorhombic commensurate phase. Finally, iii), pressure can increase interlayer interaction, which further destabilizes the orthorhombic (type II) phase relative to the hexagonal (type I) phase. The model produces a P-T phase diagram in qualitative agreement with Fig. 9. Further structural measurements will be necessary to test the model.

Acknowledgement: I am grateful for discussions with R. M. Fleming, D. E. Moncton and A. H. Moudden which served to clarify parts of this review. Supported by The Division of Materials Sciences U.S. Department of Energy under contract DE-AC02-76CH00016.

References:

[1] G. Theodorou and T.M. Rice, Phys. Rev. B18, 2840 (1978); G. Theodorou, Solid State Commun. 33, 561 (1980).

[2] J.P. Pouget, G. Shirane, J.M. Hastings, A.J. Heeger and A.G. MacDiarmid, Phys. Rev. B18, 3645 (1978); J.M. Hastings, J.P. Pouget, G. Shirane, A.J. Heeger, N.D. Miro and A.G. MacDiarmid, Phys. Rev. Lett. 39, 1484 (1977).

[3] I.U. Heilmann, J.M. Hastings, G. Shirane, A.J. Heeger and A.G. MacDiarmid, Solid State Commun. 29, 469 (1979).

[4] I.U. Heilmann, J.D. Axe, J.M. Hastings, G. Shirane, A.J. Heeger and A.G. MacDiarmid, Phys. Rev. B20, 751 (1979).

[5] J.D. Axe and P. Bak, submitted to Phys. Rev. B.

[6] V.J. Emery and J.D. Axe, Phys. Rev. Lett. 40, 1507 (1978).

[7] H. Futama, Y. Shiozaki, A. Chiba, E. Tanaka, T. Mitsui and J. Furuichi, Phys. Lett. 25A, 8 (1967).

[8] M.M. Elcombe and J.C. Taylor, Acta. Cryst. A24, 410 (1968).

[9] Y. Shiozaki, Ferroelectrics 2, 245 (1971).

[10] A.H. Moudden, F. Denoyer, M. Lambert, W. Fitzgerald, Solid State Commun. 32, 933 (1979); F. Denoyer, A.H. Moudden, M. Lambert, Ferroelectrics 24, 43 (1980).

[11] F. Denoyer, A.H. Moudden, R. Currat, C. Vettier, A. Bellamy and M. Lambert, Phys. Rev. B25, 1697 (1982).

[12] J.P. Jamet, P. Lederer and A.H. Moudden, Phys. Rev. Lett. 48, 442 (1982).

[13] A.H. Moudden, E.C. Svensson and G. Shirane, submitted to Phys. Rev. Letters.

[14] For a review of early work see J.A. Wilson, F.J. DiSalvo and S. Mahajan, Adv. Phys. 24, 117 (1975).

[15] D.E. Moncton, J.D. Axe, and F.J. DiSalvo, Phys. Rev. Lett. 34, 734 (1975); ibid, Phys. Rev. B16, 801 (1977).

[16] R.M. Fleming, D.E. Moncton, D.B. McWhan, and F.J. DiSalvo, Phys. Rev. Lett. 45, 576 (1980).

[17] P. Bak, D. Mukamel, J. Villain, and K. Wentowska, Phys. Rev. B19, 1610 (1979).

[18] K.K. Fung, S. McKernan, J.W. Steeds and J.A. Wilson, J. Phys. C14, 5417 (1981).

[19] C.H. Chen, J.M. Gibson and R.M. Fleming, Phys. Rev. Lett. 47, 723 (1981).

[20] M.B. Walker and A.E. Jacobs, Phys. Rev. B24, 6770 (1981).

[21] P.B. Littlewood and T.M. Rice, Phys. Rev. Lett. 48, 27 (1981).

[22] B.H. Suits, S. Couterie and C.P. Slichter, Phys. Rev. B23, 5142 (1981).

[23] L. Pfeiffer, quoted in ref. [7].

[24] W.L. McMillan, Phys. Rev. B14, 1496 (1976).

[25] M.B. Walker and A.E. Jacobs, Phys. Rev. B25, 3424 (1982).

[26] D.B. McWhan, R.M. Fleming, D.E. Moncton and F.J. DiSalvo, Phys. Rev. Lett. 45, 269 (1980).

[27] D.B. McWhan, J.D. Axe and R. Youngblood, Phys. Rev. B24, 5391 (1981).

Figure Captions.

1. The structure of $Hg_{3-\delta}AsF_6$.
2. Variation of velocity of long wavelength gapless excitations in $Hg_{3-\delta}AsF_6$. (Ref. 5). Symbols denote nature of mode in high symmetry direction.
3. Quasi-degenerate shear modes in $Hg_{3-\delta}AsF_6$. In case (a) both Hg sublattices are tightly coupled to the shear of the AsF_6 sublattice. In case (b) only one Hg sublattice is coupled.
4. Phase diagram of thiourea. (After Denoyer et. al. (Ref. 11)).
5. Incommensurability, $\delta(T)$, for thiourea. An applied E field causes lock-in at $\delta=1/8$. (After Moudden et. al (Ref. 13)).
6. Temperature dependence of incommensurability, δ, in 2H $TaSe_2$. On cooling only the fully incommensurate phase appears. On warming an additional stripe phase is present between $T_{CS}=93K$ and $T_{SI}=112K$.
7. Three possible commensurate phases resulting from different choices of phase for the 3 CDW components in a single layer of $2HTaSe_2$. Atomic positions are projected onto a single plane parallel to the layer. Solid lines represent maxima of the CDW's. (After Walker and Jacobs (Ref. 20)).
8. Stripe images obtained by dark field electron microscopy in 2H $TaSe_2$ at T=97K. Chen et. al. (Ref. 19).
9. P-T phase diagram for 2H $TaSe_2$. Closed circles are from neutron scattering. Other symbols are from x-ray studies (Ref. 27).

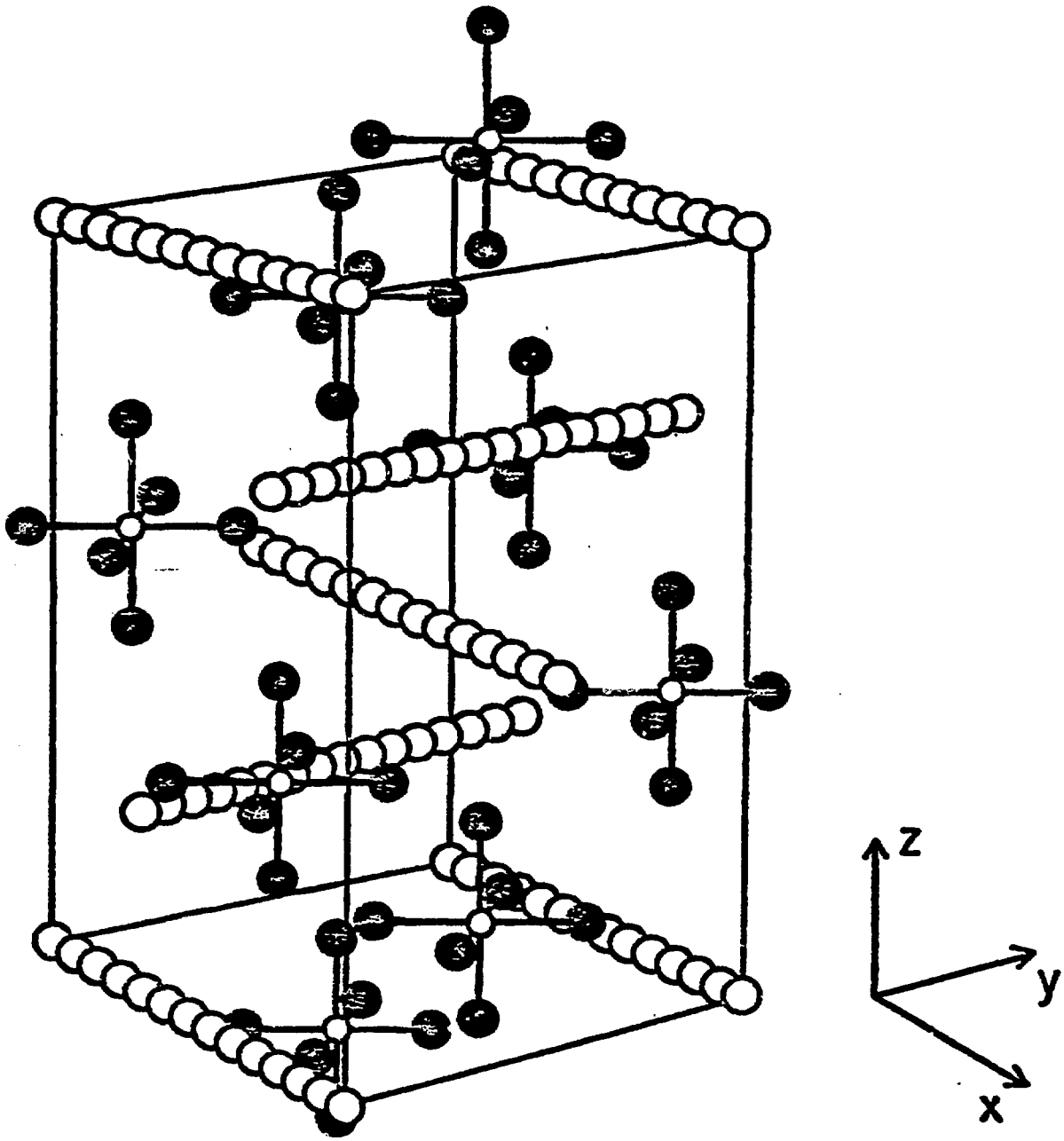

Figure 1

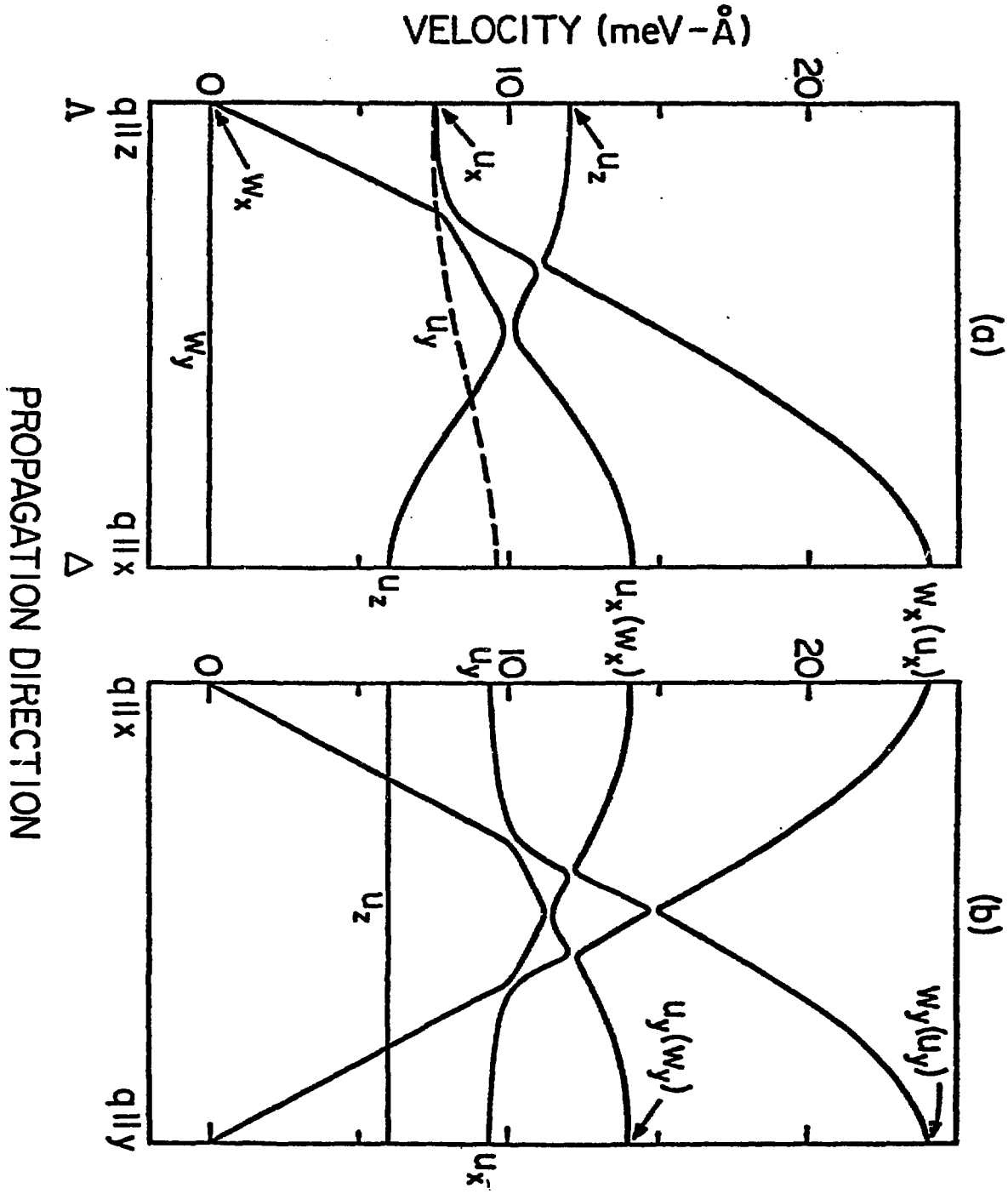
VELOCITY (meV-Å)
0
10
20
(a)
(b)
PROPAGATION DIRECTION
q||z
q||x
q||y
Λ
Δ
w_x
w_y
u_x
u_y
u_z
$w_x(u_x)$
$u_x(w_x)$
$w_y(u_y)$
$u_y(w_y)$

Figure 2

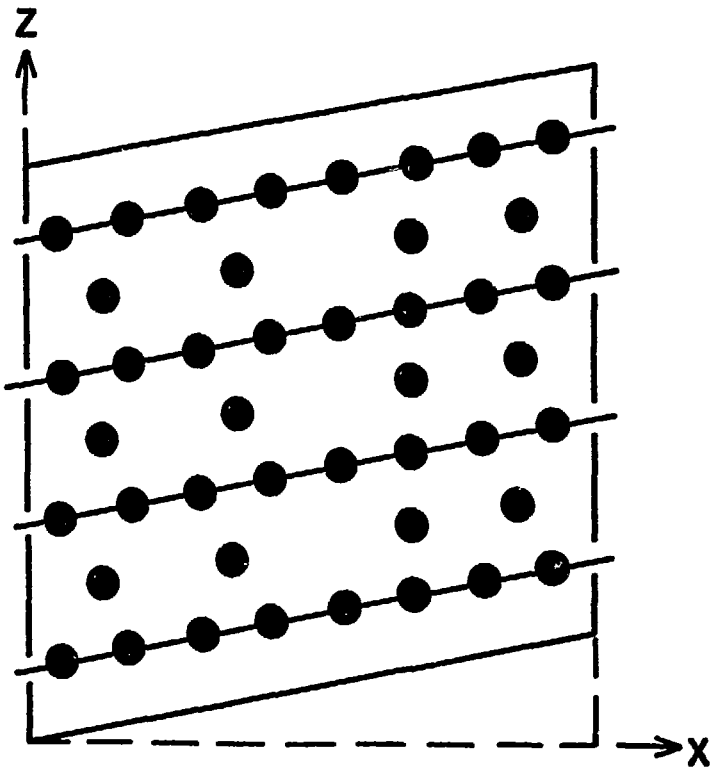

$\partial_x u_z$

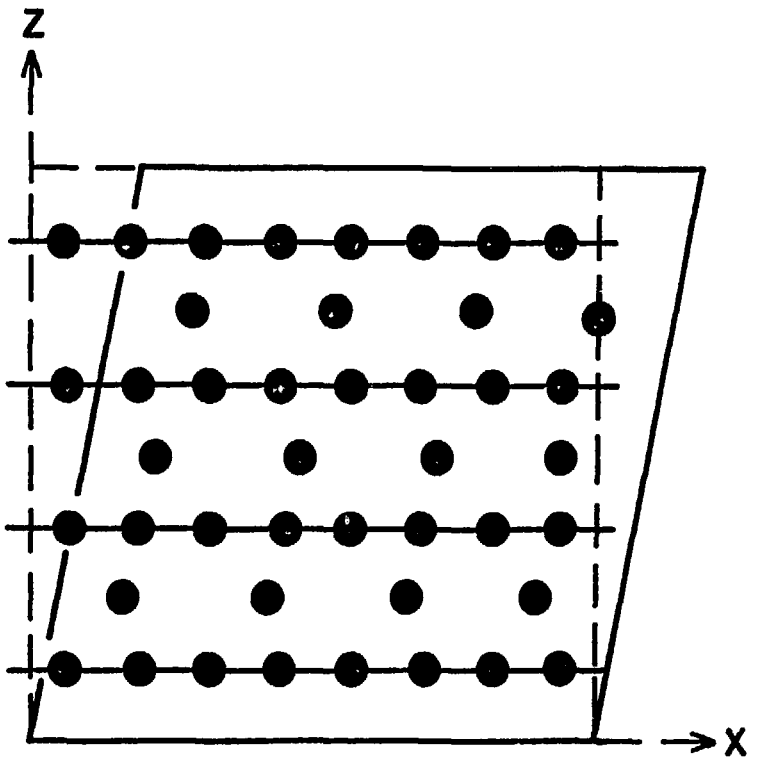

$\partial_z u_x$

Figure 3

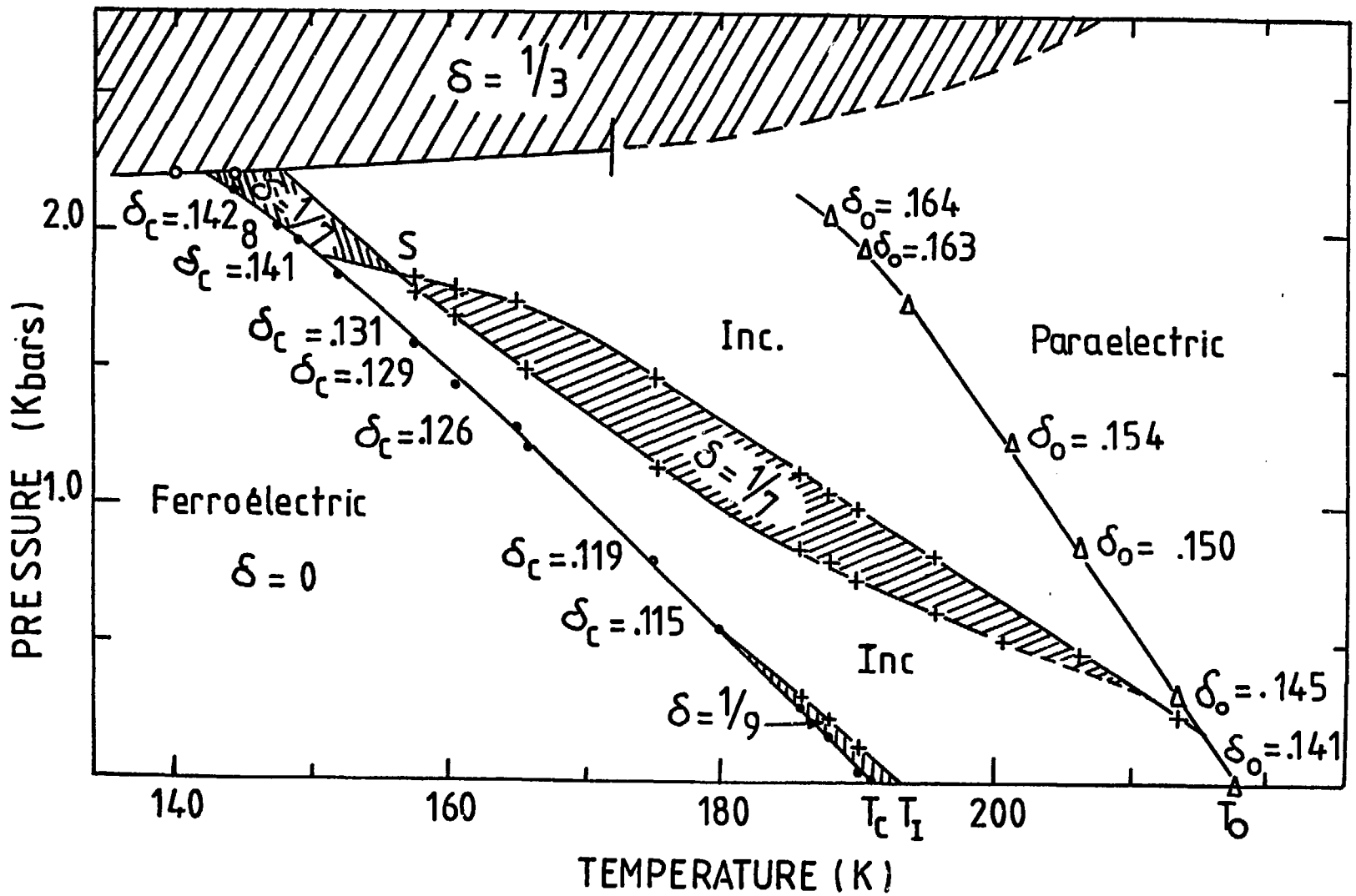
δ = 1/3
δ = 1/7
δ = 1/9
δc = .1428
δc = .141
δc = .131
δc = .129
δc = .126
δc = .119
δc = .115
δo = .164
δo = .163
δo = .154
δo = .150
δo = .145
δo = .141
S
Inc.
Inc
Paraelectric
Ferroelectric
δ = 0
2.0
1.0
PRESSURE (Kbars)
140
160
180
200
Tc
TI
To
TEMPERATURE (K)

Figure 4

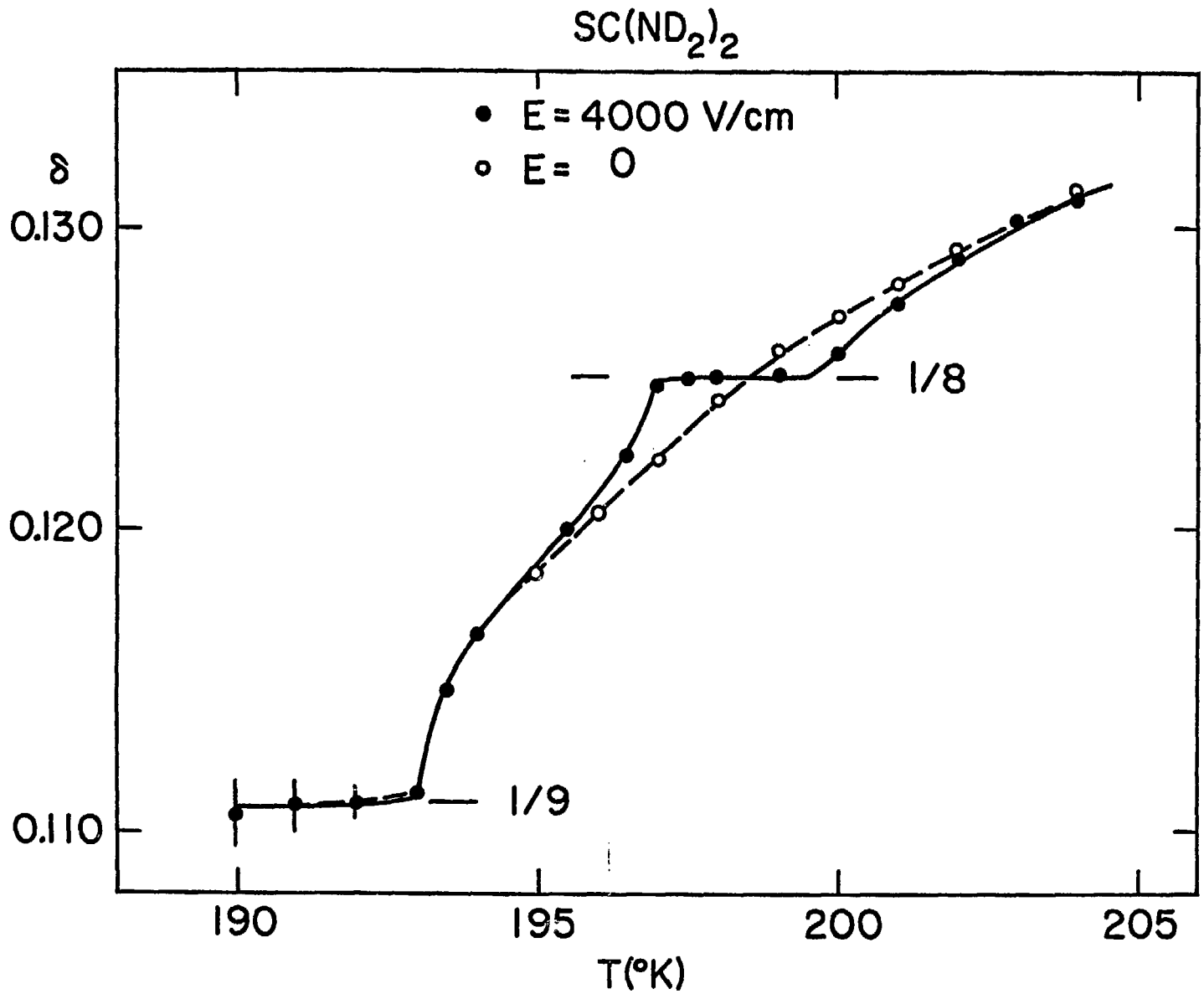

Figure 5

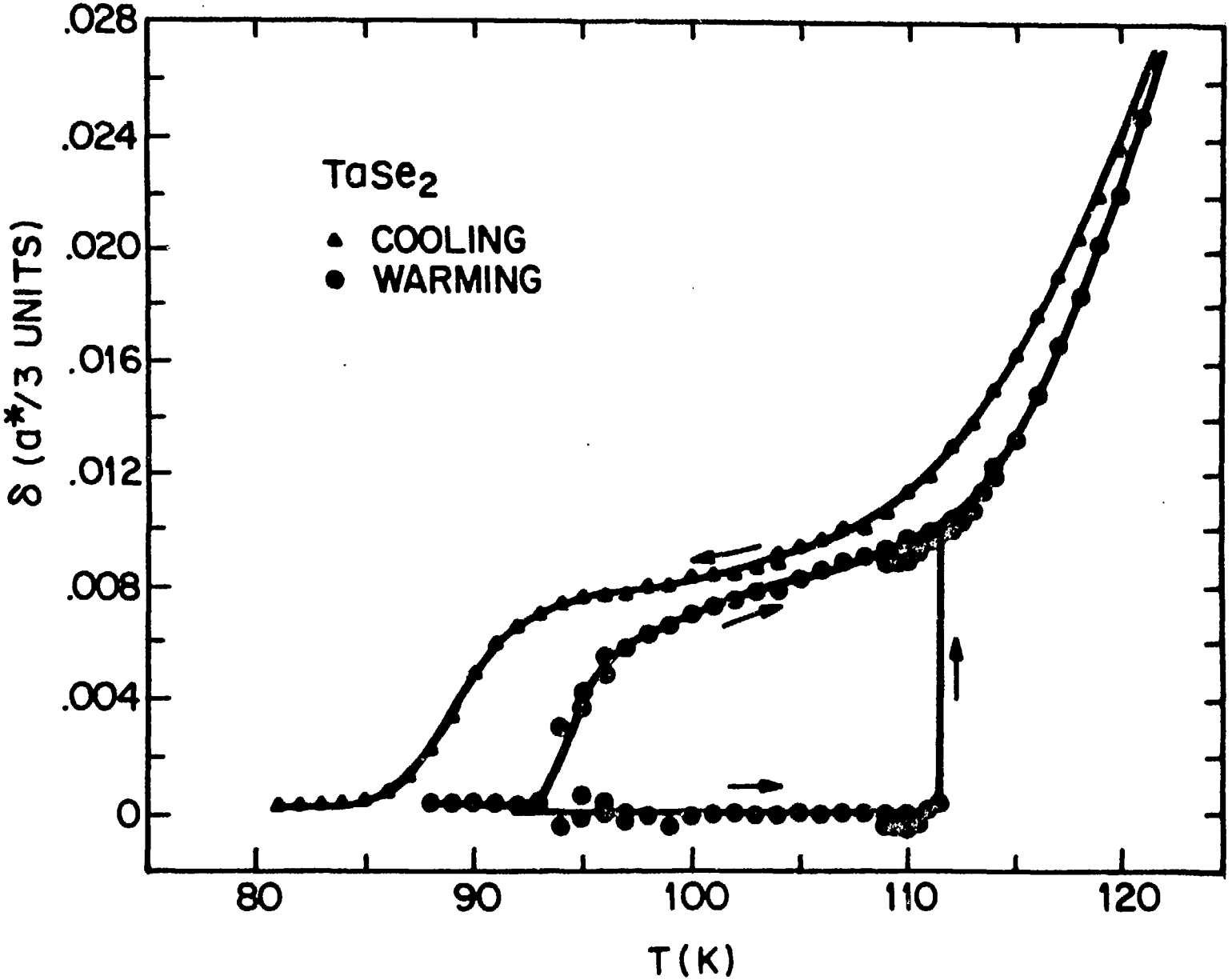
TaSe2
COOLING
WARMING
δ (a*/3 UNITS)
.028
.024
.020
.016
.012
.008
.004
0
80
90
100
110
120
T(K)

Figure 6

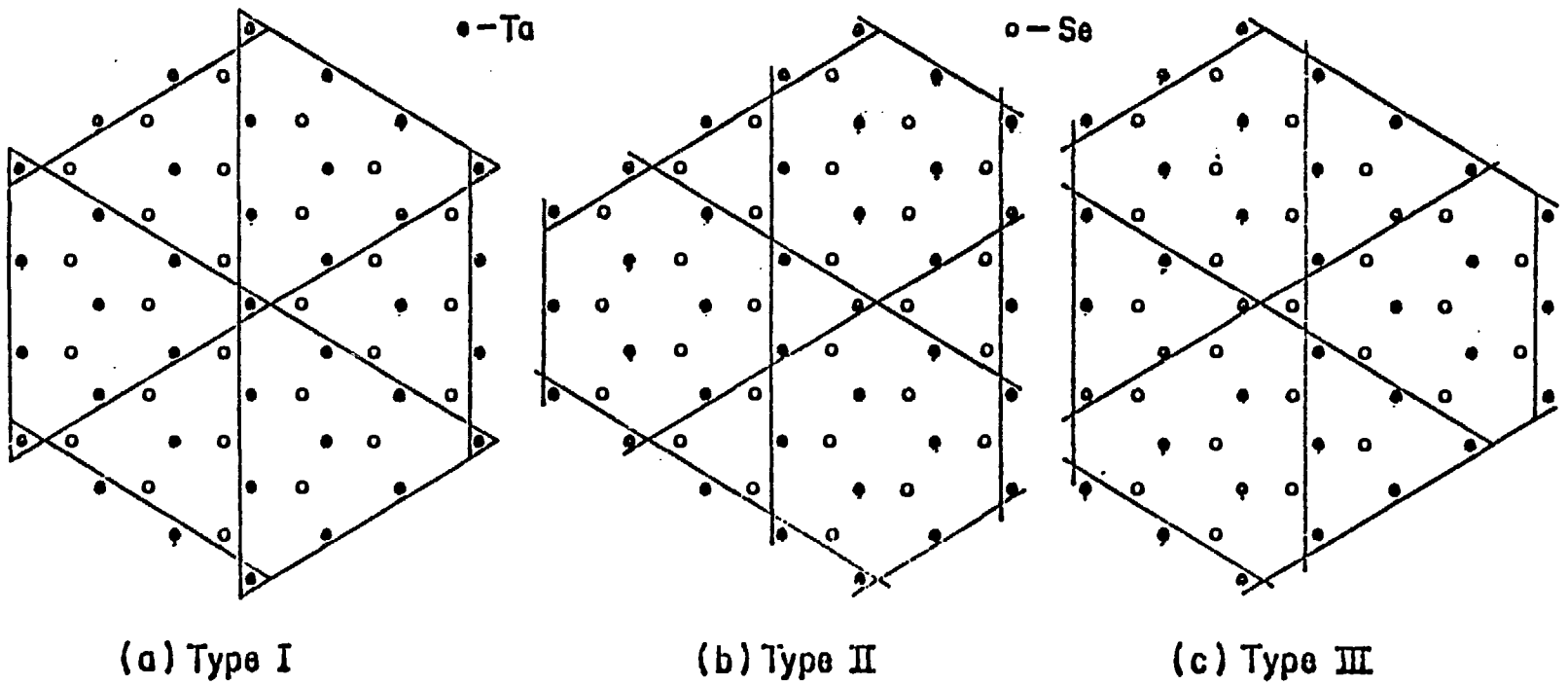

Figure 7

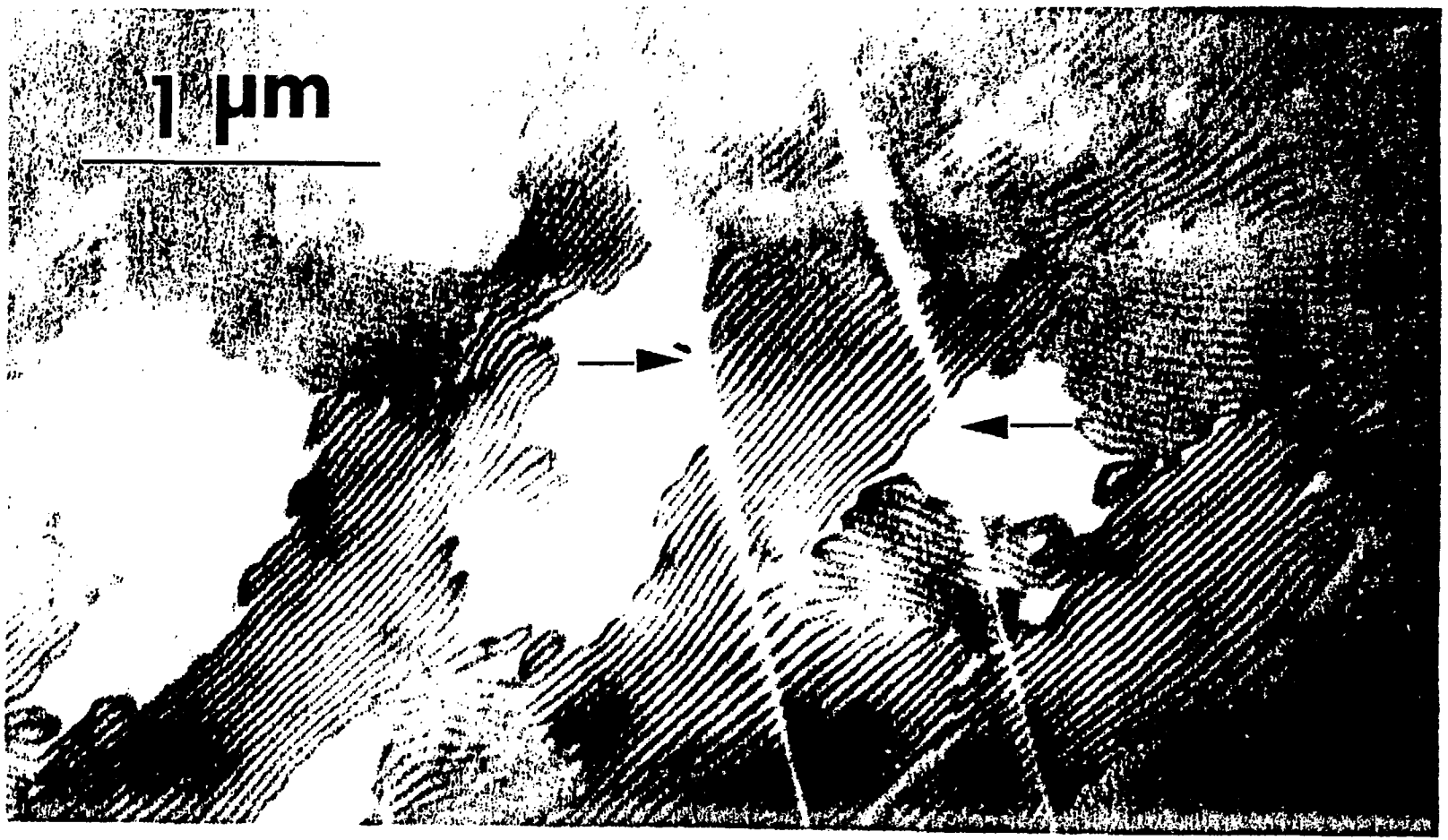

Figure 8

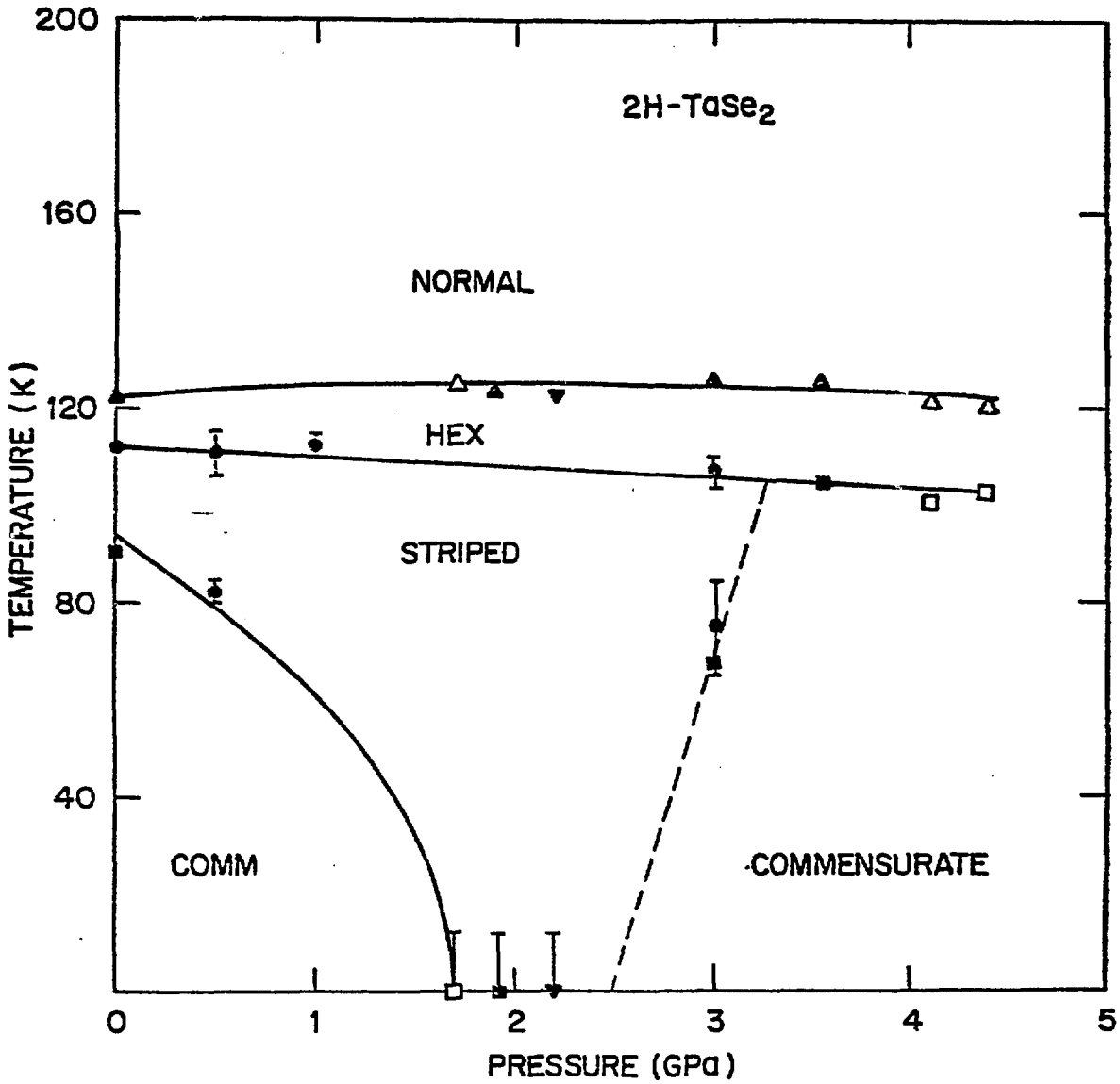
2H-TaSe2
NORMAL
HEX
STRIPED
COMM
COMMENSURATE
TEMPERATURE (K)
PRESSURE (GPa)
200
160
120
80
40
0
1
2
3
4
5

Figure 9